PCCP

PAPER

Photoelectron spectroscopy and density functional study of $Co_nC_2^-$ (n = 1–5) clusters†

Cite this: *Phys. Chem. Chem. Phys.*, 2014, **16**, 5434

Jin-Yun Yuan,[ab] Hong-Guang Xu[a] and Wei-Jun Zheng*[a]

Received 11th November 2013,
Accepted 18th December 2013

DOI: 10.1039/c3cp54758b

www.rsc.org/pccp

$Co_nC_2^-$ (n = 1–5) cluster anions were investigated using anion photoelectron spectroscopy. The adiabatic detachment energies (ADEs) and the vertical detachment energies (VDEs) of the $Co_nC_2^-$ (n = 1–5) cluster anions were determined from their photoelectron spectra. Density functional calculations were performed for the Co_nC_2 (n = 1–5) cluster anions and neutrals. Our studies show that the structures of $Co_nC_2^-$ (n = 1–5) can be described as attaching C_2 to the top sites, bridge sites, or hollow sites of the Co_n clusters. The C_2 retains an integral structure unit in the Co_nC_2 (n = 1–5) cluster anions and neutrals, rather than being separated by the Co_n clusters. The C_2 unit in the Co_nC_2 (n = 1–5) cluster anions and neutrals has the characteristics of a double-bond.

I. Introduction

Metal carbide compounds have received a great deal of attention because they present versatile applications in the electric, magnetic, mechanic and catalytic fields.[1,2] Small metal carbide clusters are useful models for providing insight into the growth mechanisms of metal–carbon nanomaterials, therefore, a lot of effort has been devoted to studying small $M_{1-2}C_2$ clusters in experiments and theory.[3–13] Photoelectron spectroscopy studies of MC_2^- (M = Sc, V, Cr, Mn, Fe and Co) have suggested that the M–C_2 and M–O interactions are similar and MC_2 can be qualitatively viewed as ionic $M^{2+}C_2^{2-}$.[14] The theoretical calculations of Jena and coworkers have predicted the structure of the FeC_2 cluster to be cyclic.[15] The calculations of Tran *et al.*[16,17] have suggested that the experimental photoelectron spectrum features of MnC_2^- are contributed by its cyclic isomer while those of CrC_2^- are contributed by both the cyclic and linear isomers. Some small $M_{1-2}C_2$ clusters and the encapsulation of M_xC_2 (x = 2–4, M = Sc, Y, Ti, Gd) in fullerene carbon cages have also been investigated experimentally and theoretically.[18–23] However, investigation on multi-metal dicarbon clusters is very rare. On the other hand, it has been reported that the cobalt-catalyzed carbon nanotubes have single-atomic-layer walls, differing from the nanotubes catalyzed by Fe, Ni or a Ni:Cu mixture.[24] However, it is unclear how cobalt was able to catalyze the formation of these single-walled tubes. Investigations of cobalt carbide may provide some insight into the formation mechanism of the cobalt-catalyzed carbon nanotube. In this work, we studied $Co_nC_2^-$ (n = 1–5) cluster anions by combining photoelectron spectroscopy and Density Functional Theory (DFT) calculations.

II. Experimental and theoretical methods

A. Experimental method

The experiments were conducted on a home-built apparatus consisting of a time-of-flight mass spectrometer and a magnetic-bottle photoelectron spectrometer, which has been described elsewhere.[25] Briefly, the $Co_nC_2^-$ (n = 2–5) cluster anions were generated in a laser vaporization source by laser ablation of a rotating, translating disk target (13 mm diameter, graphite/Co mol ratio 40 : 1) with the second harmonic (532 nm) of a Nd:YAG laser (Continuum Surelite II-10). Helium gas with ~4 atm backing pressure was allowed to expand through a pulsed valve into the source to cool the formed clusters. Because the intensity of CoC_2^- cluster anion is quite low using the above-mentioned method, the CoC_2^- cluster anions were produced by laser ablation of a cobalt target and an expanding helium carrier gas of ~4 atm backing pressure seeded with ethene molecules (~0.1%). The cluster anions of interest were each mass-selected and decelerated before being photodetached by the second (532 nm) and fourth harmonic (266 nm) of a second Nd:YAG laser. The resultant electrons were energy-analyzed by the magnetic-bottle photoelectron spectrometer. The energy resolution of the photoelectron spectrometer was approximately 40 meV at the electron kinetic energy of 1 eV. The photoelectron spectra were calibrated using the spectrum of Cu^- taken at similar conditions.

[a] *Beijing National Laboratory for Molecular Sciences, State Key Laboratory of Molecular Reaction Dynamics, Institute of Chemistry, Chinese Academy of Sciences, Beijing 100190, China. E-mail: zhengwj@iccas.ac.cn*

[b] *Institute of Nanostructured Functional Materials, Huanghe Science and Technology College, Zhengzhou, Henan 450006, China*

† Electronic supplementary information (ESI) available: Cartesian coordinates of Co_nC_2 (n = 1–5) clusters, anions and neutrals in the article are collected in the ESI. See DOI: 10.1039/c3cp54758b

B. Theoretical method

The structural optimization and frequency calculations were carried out with Density Functional Theory (DFT) using the pure functional BPW91[26,27] and the 6-311+G(d) basis set, as implemented in the Gaussian03 program package.[28] In order to test the reliability of our calculations, the electron affinity of CoC_2 was also calculated employing the hybrid functionals B3LYP[29,30] and B3PW91[29] in combination with the 6-311+G(d) basis set. It was found that the result from the pure functional BPW91 (1.87 eV) is in better agreement with the experimental value (1.74 eV) than those of the hybrid functionals B3LYP (2.03 eV) and B3PW91 (1.92 eV). Thus, the BPW91 functional was used in this work. During the calculations, the initial structures of the $Co_nC_2^-$ (n = 1–5) clusters were optimized at all possible spin multiplicities until the geometric structures of energy-minima were obtained. Harmonic vibrational frequencies were calculated to make sure that the optimized structures correspond to the real local minima. The zero-point vibrational energies and spin contamination were considered for all stable isomers.

III. Experimental results

The photoelectron spectra of $Co_nC_2^-$ (n = 1–5) taken with 266 nm photons are shown in Fig. 1. The spectra of $Co_nC_2^-$ (n = 2–4) taken with 532 nm photons are shown in Fig. 2. The vertical detachment energies (VDEs) and the adiabatic detachment energies (ADEs) of the cluster anions estimated from the photoelectron spectra are listed in Table 1. The ADE from each spectrum was determined by adding the value of the instrumental resolution to the onset of the first peak in the photoelectron spectra. The onset of the first peak was determined by drawing a straight line along the leading edge of the first peak to cross the baseline of the spectra.

The photoelectron spectrum of CoC_2^- at 266 nm has a broad peak centered at ~2.03 eV and a sharp peak centered at ~2.65 eV, followed by a broad peak centered at ~3.13 eV. The spectrum of CoC_2^- in our experiments is consistent with the previous spectrum of CoC_2^- taken by Li *et al.*[14] except that the relative intensities of the peaks are different due to different photodetachment cross-sections at 266 nm and 355 nm. In the spectrum of $Co_2C_2^-$ at 266 nm, there is an intense peak in the range 1.6–2.0 eV and several broad peaks at the high binding energy side above 2.0 eV. The top of the first peak is determined more precisely to be 1.75 eV in the spectrum at 532 nm. $Co_3C_2^-$ has one resolved feature centered at ~1.92 eV and another very broad unresolved feature beyond 2.0 eV. The spectrum of $Co_4C_2^-$ at 266 nm shows a strong peak centered at ~2.52 eV and several small peaks in the range 2.8–3.4 eV. In addition, it also has a long tail at the low binding energy side in the range 1.4–2.0 eV as can be seen in the spectrum at 532 nm, which may come from the excited states or the other isomers of $Co_4C_2^-$ produced with low abundance. The spectrum of $Co_5C_2^-$ contains two major peaks centered at ~2.37 and 2.81 eV and a small peak at ~2.07 eV. Some peaks are also observed between 3.0 eV and 3.6 eV.

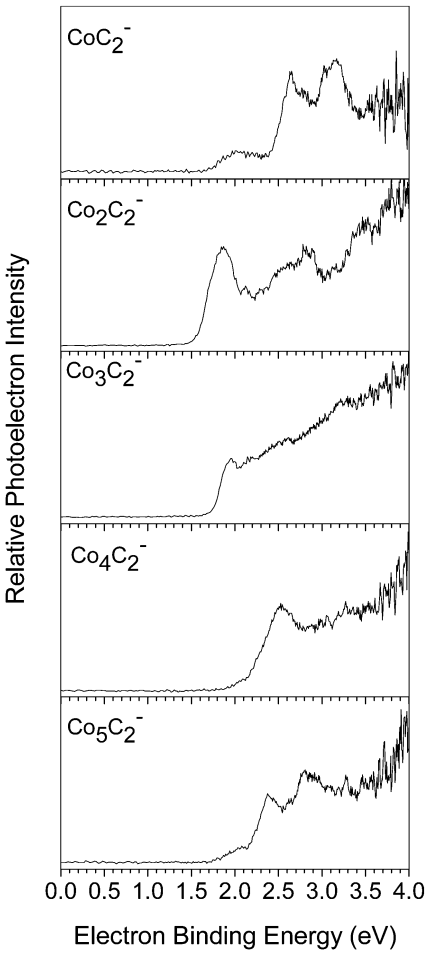

Fig. 1 Photoelectron spectra of $Co_nC_2^-$ (n = 1–5) cluster anions recorded with 266 nm photons.

IV. Theoretical results and discussion

The optimized geometries of the low-lying isomers of the $Co_nC_2^-$ (n = 1–5) cluster anions obtained with DFT calculations are presented in Fig. 3 with the most stable ones on the left. Various initial structures were considered in the calculations, such as inserting Co atoms between the two carbon atoms or attaching a Co atom directly to one end of the C_2 dimer. It is found that these structures are less stable than the structures with the C_2 dimer adsorbed directly on the Co_n (n = 1–5) clusters as shown in Fig. 3.

The structures of the neutral Co_nC_2 (n = 1–5) clusters were also optimized using their corresponding anion structures as initial structures. The most stable isomers of the Co_nC_2 (n = 1–5) cluster neutrals are presented in Fig. 4. Based on the energy differences between the neutrals (optimized using the anionic structures as initial structures) and the anions, we calculated the ADEs of these isomers. The VDEs of the cluster anions were calculated based on the energy differences between the neutrals and the anions with the neutrals at the geometries of their corresponding anionic species. For the anionic clusters with multiplicity M, the neutral species with multiplicities

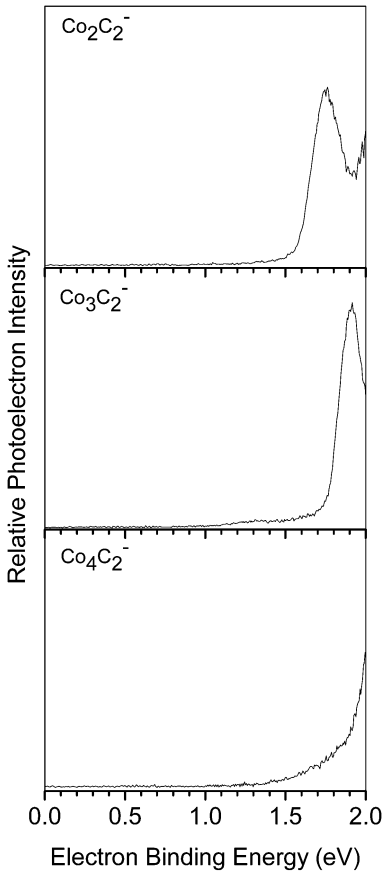

Fig. 2 Photoelectron spectra of $Co_nC_2^-$ (n = 2–4) cluster anions recorded with 532 nm photons.

Table 1 Experimentally observed VDEs and ADEs (eV) from the photoelectron spectra of $Co_nC_2^-$ (n = 1–5) with 532 and 266 nm photons[a]

Cluster	ADE	VDE
CoC_2^-	1.74	2.03
$Co_2C_2^-$	1.61	1.75
$Co_3C_2^-$	1.80	1.92
$Co_4C_2^-$	1.93	2.52
$Co_5C_2^-$	1.83	2.07

[a] The uncertainties of the experimental values are ±0.08 eV.

$M-1$ and $M+1$ were considered in the VDE and ADE calculations. The calculated VDEs, ADEs and relative energies of the low-lying isomers of the $Co_nC_2^-$ (n = 1–5) cluster anions are listed in Table 2 along with the experimental values for comparison.

A. CoC_2^-

The most stable isomer of the CoC_2^- cluster is 1A which is an isosceles triangular structure in the triplet state. The C–C bond distance of isomer 1A is ~1.33 Å, the same as that in a free ethene molecule (1.33 Å).[31] The C–Co bond distances are both 1.86 Å, very close to that of the C–Co covalent bond (1.83 Å),[32] indicating that the Co and C atoms form covalent bonds in CoC_2^-. The theoretical VDE of isomer 1A is 1.87 eV, in reasonable agreement with the experimental VDE (2.03 eV) of CoC_2^-. The calculated ADE of isomer 1A is 1.87 eV, close to the experimental value (1.74 eV) obtained in this work and ref. 14 (1.7 eV). Isomer 1B is a linear structure with $C_{\infty v}$ symmetry. The theoretical VDE (2.24 eV) of isomer 1B is close to the experimental value (2.03 eV), but it is 0.24 eV energetically above isomer 1A. Isomer 1C is higher in energy than isomer 1A by 0.43 eV and its theoretical VDE is inconsistent with the experimental measurement. The calculated Co–C_2 stretching frequency of the neutral isomer calculated based on isomer 1A is about 563 cm^{-1}, which is in good agreement with the experimental measurement (~540 cm^{-1}) by Li *et al.*[14] This fact may be the reason that the first peak of CoC_2^- is broad. Therefore, the experimental spectrum features of CoC_2^- are probably contributed by isomer 1A.

B. $Co_2C_2^-$

The first two isomers (2A and 2B) of the $Co_2C_2^-$ cluster are nearly degenerate in energy, with isomer 2B higher than isomer 2A by only 0.01 eV. The electronic states of isomers 2A and 2B are $^6A''$ and $^4A'$, respectively. They both have a planar four-member structure. The C–C bond distances of isomers 2A and 2B are calculated to be 1.31 and 1.32 Å, respectively, very close to that of CoC_2^- (1.33 Å). The calculated VDE of isomer 2A (1.54 eV) is in better agreement with the experimental values (1.75 eV) than that of isomer 2B (1.41 eV). The calculated VDE of isomer 2C is close to that of isomer 2A, but it is 0.25 eV higher in energy than isomer 2A, so its existence in the experiment can be ruled out. Therefore, we suggest that isomer 2A is the probable ground state structure. Using photoelectron spectroscopy and theoretical calculations, Tono *et al.* also reported that isomer 2A is the ground state structure of the $Co_2C_2^-$ cluster.[12]

C. $Co_3C_2^-$

The most stable isomer of the $Co_3C_2^-$ cluster (3A) has a non-planar five-member ring structure with a ^7A electronic state. Isomer 3A may be formed by attaching a cobalt atom to the four-member $Co_2C_2^-$ cluster through two Co–Co interactions. The C–C bond distance of isomer 3A is 1.30 Å, close to that of the ethene molecule (1.33 Å). The theoretical VDE of isomer 3A is 1.89 eV, in good agreement with that of the experimental measurement (1.92 eV). Isomers 3B, 3C and 3D are 0.33, 0.35 and 0.35 eV higher in energy than isomer 3A, respectively. The VDEs of these three isomers deviate far from the experimental value. Therefore, we suggest that isomer 3A is the most probable structure of $Co_3C_2^-$.

D. $Co_4C_2^-$

The first five stable isomers of the $Co_4C_2^-$ cluster (4A–4E) are nearly degenerate in energy, with energy differences of only 0.05, 0.06, 0.06, and 0.06 eV. The structures of isomers 4A and 4C are both composed of a distorted tetrahedral Co_4 cluster adsorbing the C_2 dimer on its surface. Isomer 4B is a structure with a butterfly-like Co_4 cluster adsorbing the C_2 dimer on a Co–Co bond. Isomer 4D is a structure with a distorted tetrahedral Co_4 cluster adsorbing the C_2 dimer on a Co–Co bond. Isomer 4E can be considered as isomer 3B face-capped by a Co atom. Isomers 4F, 4G and 4H are 0.14, 0.20 and 0.22 eV higher

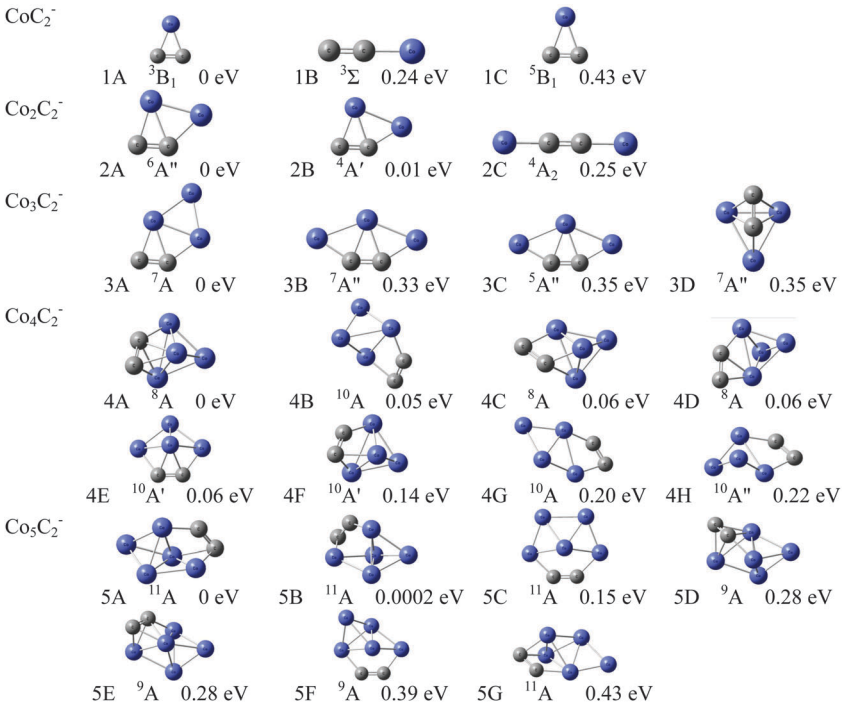

Fig. 3 Low-lying isomers of $Co_nC_2^-$ (n = 1–5) cluster anions.

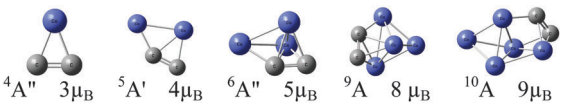

Fig. 4 The most stable isomers of Co_nC_2 (n = 1–5) neutrals.

in energy than isomer 4A. The calculated VDEs of isomers 4B, 4D, 4G and 4H are 2.32, 2.28, 2.41 and 2.24 eV, respectively, which are all close to the experimental VDE (2.52 eV) of $Co_4C_2^-$. Hence, isomers 4B, 4D, 4G and 4H might be all the probable species detected in the experiments. Since the spectrum of the $Co_4C_2^-$ cluster at 532 nm exhibits a long tail at roughly 2.0 eV, which covers the VDEs of isomers 4A, 4C, 4E, and 4F (1.90, 2.13, 2.02 and 2.14 eV), we suggest that these weak features are likely to be contributed by isomers 4A, 4C, 4E, and 4F.

E. $Co_5C_2^-$

Isomers 5A and 5B are nearly degenerate in energy. They have a similar structure with a distorted bi-pyramidal Co_5 cluster adsorbing the C_2 dimer on its surface in different directions. Isomer 5C is a capped six-member ring structure with a non-planar W-like Co_5 cluster adsorbing the C_2 dimer. It is only 0.15 eV energetically above isomer 5A. The theoretical VDEs of isomers 5A, 5B and 5C are in good agreement with the experimental measurements. Thus, we suggest that isomers 5A–5C coexist in our experiment. Isomers 5D and 5E are both 0.28 eV higher in energy than isomer 5A. Their calculated VDEs are not in accordance with the experimental values. Although the calculated VDEs of isomers 5F and 5G are close to the experimental measurement, they are much higher in energy than isomer 5A. So we suggest that the existence of isomers 5D–5G in the experiments can be excluded.

Table 2 Relative energies (RE) of the low-lying isomers of $Co_nC_2^-$ (n = 1–5) as well as their VDEs and ADEs obtained by density functional calculations

					VDE (eV)		ADE (eV)	
Isomer		State	Sym.	RE (eV)	Theo.	Expt.	Theo.	Expt.
CoC_2^-	1A	$^3B_1$	C_{2v}	0	1.87	2.03	1.87	1.74
	1B	$^3\Sigma$	$C_{\infty v}$	0.24	2.24		1.63	
	1C	$^5B_1$	C_{2v}	0.43	1.49		1.44	
$Co_2C_2^-$	2A	$^6A''$	C_s	0	1.54	1.75	1.41	1.61
	2B	$^4A'$	C_s	0.01	1.41		1.40	
	2C	$^4A_2$	C_{2v}	0.25	1.50		1.50	
$Co_3C_2^-$	3A	^7A	C_1	0	1.89	1.92	1.84	1.80
	3B	$^7A''$	C_s	0.33	1.48		1.37	
	3C	$^5A''$	C_s	0.35	1.43		1.35	
	3D	$^7A''$	C_s	0.35	1.33		1.26	
$Co_4C_2^-$	4A	^8A	C_1	0	1.90	2.52	1.83	1.93
	4B	^{10}A	C_1	0.05	2.32		2.29	
	4C	^8A	C_1	0.06	2.13		1.94	
	4D	^8A	C_1	0.06	2.28		2.20	
	4E	$^{10}A'$	C_s	0.06	2.02		2.00	
	4F	$^{10}A'$	C_s	0.14	2.14		2.11	
	4G	^{10}A	C_1	0.20	2.41		2.32	
	4H	$^{10}A''$	C_s	0.22	2.24		2.13	
$Co_5C_2^-$	5A	^{11}A	C_1	0	2.00	2.07	1.88	1.83
	5B	^{11}A	C_1	0.0002	2.00		1.88	
	5C	^{11}A	C_1	0.15	1.98		1.94	
	5D	^9A	C_1	0.28	1.64		1.60	
	5E	^9A	C_1	0.28	1.64		1.60	
	5F	^9A	C_1	0.39	1.73		1.62	
	5G	^{11}A	C_1	0.43	1.87		1.45	

From Fig. 3 and 4, we can observe that the transitions from the two-dimensional to the three-dimensional structures of the Co_nC_2 cluster anions and neutrals both occur at n = 3. The neutral structures of Co_nC_2 (n = 1–5) vary only slightly from their corresponding anions except for n = 3. In the $Co_3C_2^-$ cluster anion, the C_2 dimer is adsorbed on an edge of the triangular Co_3 cluster, whereas it is adsorbed on the surface of the triangular Co_3 cluster in the corresponding Co_3C_2 neutral cluster. The C–C distances of the Co_nC_2 (n = 1–5) cluster anions and neutrals are in the range 1.30–1.36 Å, very close to that of the C=C bond (1.33 Å) in an ethene molecule,[31] indicating that carbon–carbon bonds in the Co_nC_2 clusters possess the double bond character. The C_2 retains an integral structure unit in the Co_nC_2 (n = 1–5) cluster anions and neutrals, rather than being separated by the Co_n clusters. As carbon nanotubes can be generated by assembling many C_2 units, the formation of C_2 on cobalt is probably related to the formation of single-walled carbon nanotubes catalyzed by cobalt.

It has been reported that the magnetic moments of bare Co_n (n = 1–5) clusters are 3 μ_B, 4 μ_B, 5 μ_B (or 7 μ_B), 8 μ_B (or 10 μ_B), and 11 μ_B (or 13 μ_B), respectively.[33–36] The most preferred spin states of the Co_nC_2 (n = 1–5) clusters are quartet, quintet, sextet, nonet and dectet, respectively, thus resulting in their most preferred magnetic moments of 3 μ_B, 4 μ_B, 5 μ_B, 8 μ_B, and 9 μ_B, respectively as shown in Fig. 4. It can be seen that the magnetic moments of the Co_nC_2 (n = 1–5) clusters are similar to those of bare Co_n (n = 1–5) clusters and increase with the addition of a Co atom. Thus, we suggest that Co_nC_2 clusters may be excellent magnetic materials like the bare Co_n cluster.

It would be interesting to compare Co_nC_2 with Co_nC_2H (n = 1–5) clusters which have been previously investigated by anion photoelectron spectroscopy and DFT calculations.[37] The magnetic moments of the Co_nC_2H and Co_nC_2 (n = 1–5) clusters are both similar to the bare Co_n (n = 1–5) clusters. The characters of the carbon–carbon bonds in the Co_nC_2H and Co_nC_2 (n = 1–5) clusters are very different. It can be seen that the carbon–carbon bonds of Co_nC_2H (n = 1–5) are more similar to the C≡C bond of acetylene, whereas the C–C bonds in the Co_nC_2 (n = 1–5) clusters are more similar to the C=C bond in ethene. The VDEs of the $Co_nC_2^-$ (n = 1–5) cluster anions are all higher than those of corresponding $Co_nC_2H^-$ (n = 1–5) cluster anions, which may be due to the electron affinity of C_2 (3.27 eV) being larger than that of C_2H (2.97 eV).[38]

V. Conclusions

Anion photoelectron spectroscopy and density functional calculations were conducted to investigate $Co_nC_2^-$ (n = 1–5) clusters. The results show that the most stable isomers of $Co_nC_2^-$ (n = 1–5) can be considered as attaching C_2 to the top sites, bridge sites or hollow sites of the Co_n (n = 2–5) clusters. The C_2 dimer only affects the magnetic moments of the bare Co_n (n = 1–5) clusters slightly. The C–C bonds in the Co_nC_2 (n = 1–5) cluster anions and neutrals have a double bond character, which is very different from the C≡C bond in Co_nC_2H (n = 1–5) clusters.

Acknowledgements

This work was supported by the Natural Science Foundation of China (NSFC, Grant No. 21273246 and 20933008), the Natural Science Foundation of the Education Department of Henan Province (No. 13B150987) and the Natural Science Foundation of Zhengzhou City (No. 20120324). The theoretical calculations were conducted on ScGrid and DeepComp 7000 at the Supercomputing Center, Computer Network Information Center of the Chinese Academy of Sciences.

References

1 J. G. Chen, *Chem. Rev.*, 1996, **96**, 1477–1498.
2 J. Emsley, *The Elements*, Clarendon, Oxford, U.K., 1989, p. 174.
3 P. Redondo, L. Largo and C. Barrientos, *Chem. Phys.*, 2009, **364**, 1–13.
4 M. F. A. Hendrickx and S. Clima, *Chem. Phys. Lett.*, 2004, **388**, 290–296.
5 M. F. A. Hendrickx and S. Clima, *Chem. Phys. Lett.*, 2004, **388**, 284–289.
6 H. J. Zhai, S. R. Liu, X. Li and L.-S. Wang, *J. Chem. Phys.*, 2001, **115**, 5170–5178.
7 M. V. Ryzhkov, A. L. Ivanovskii and B. T. Delley, *Chem. Phys. Lett.*, 2005, **404**, 400–408.
8 N. Nishi, K. Kosugi, K. Hino, T. Yokoyama and E. Okunishi, *Chem. Phys. Lett.*, 2003, **369**, 198–203.
9 K. Tono, A. Terasaki, T. Ohta and T. Kondow, *Chem. Phys. Lett.*, 2002, **351**, 135–141.
10 N. A. Cannon, A. I. Boldyren, X. Li and L.-S. Wang, *J. Chem. Phys.*, 2000, **113**, 2671–2679.
11 R. Sumathi and M. Hendrickx, *J. Phys. Chem. A*, 1999, **103**, 585–591.
12 K. Tono, A. Terasaki, T. Ohta and T. Kondow, *J. Chem. Phys.*, 2002, **117**, 7010–7016.
13 V. M. Rayon, P. Redondo, C. Barrientos and A. Largo, *Chem.–Eur. J.*, 2006, **12**, 6963.
14 X. Li and L.-S. Wang, *J. Chem. Phys.*, 1999, **111**, 8389–8395.
15 B. K. Nash, B. K. Rao and P. Jena, *J. Chem. Phys.*, 1996, **105**, 11020–11023.
16 V. T. Tran, C. Iftner and M. F. A. Hendrickx, *Chem. Phys. Lett.*, 2013, **575**, 46–53.
17 V. T. Tran, C. Iftner and M. F. A. Hendrickx, *J. Phys. Chem. A*, 2013, **117**, 5613–5619.
18 T.-S. Wang, N. Chen, J.-F. Xiang, B. Li, J.-Y. Wu, W. Xu, L. Jiang, K. Tan, C.-Y. Shu, X. Lu and C.-R. Wang, *J. Am. Chem. Soc.*, 2009, **131**, 16646–16647.
19 M. Inakuma, E. Yamamoto, T. Kai, C.-R. Wang, T. Tomiyama, H. Shinohara, T. J. S. Dennis, M. Hulman, M. Krause and H. Kuzmany, *J. Phys. Chem. B*, 2000, **104**, 5072–5077.
20 K. Tan, X. Lu and C.-R. Wang, *J. Phys. Chem. B*, 2006, **110**, 11098–11102.
21 Y. Iiduka, T. Wakahara, T. Nakahodo, T. Tsuchiya, A. Sakuraba, Y. Maeda, T. Akasaka, K. Yoza, E. Horn, T. Kato, M. T. H. Liu,

N. Mizorogi, K. Kobayashi and S. Nagase, *J. Am. Chem. Soc.*, 2005, **127**, 12500–12501.
22 H. Yang, C. X. Lu, Z. Y. Liu, H. X. Jin, Y. L. Che, M. M. Olmstead and A. L. Balch, *J. Am. Chem. Soc.*, 2008, **130**, 17296–17300.
23 K. Tan and X. Lu, *Chem. Commun.*, 2005, 4444–4446.
24 D. S. Bethune, C. H. Klang, M. S. de Vries, G. Gorman, R. Savoy, J. Vazquez and R. Beyers, *Nature*, 1993, **363**, 605–607.
25 H.-G. Xu, Z.-G. Zhang, Y. Feng, J. Y. Yuan, Y. C. Zhao and W. J. Zheng, *Chem. Phys. Lett.*, 2010, **487**, 204–208.
26 A. D. Beck, *Phys. Rev. A: At., Mol., Opt. Phys.*, 1988, **38**, 3098.
27 J. P. Perdew and Y. Wang, *Phys. Rev. B: Condens. Matter Mater. Phys.*, 1991, **45**, 13244.
28 M. J. Frisch, G. W. Trucks, H. B. chlegel, G. E. Scuseria, M. A. Robb, J. R. Cheeseman, V. G. Zakrzewski, J. A. Montgomery, Jr., R. E. Stratmann, J. C. Burant, S. Dapprich, J. M. Millam, A. D. Daniels, K. N. Kudin, M. C. Strain, O. Farkas, J. Tomasi, V. Barone, M. Cossi, R. Cammi, B. Mennucci, C. Pomelli, C. Adamo, S. Clifford, J. Ochterski, G. A. Petersson, P. Y. Ayala, Q. Cui, K. Morokuma, D. K. Malick, A. D. Rabuck, K. Raghavachari, J. B. Foresman, J. Cioslowski, J. V. Ortiz, A. G. Baboul, B. B. Stefanov, G. Liu, A. Liashenko, P. Piskorz, I. Komaromi, R. Gomperts, R. L. Martin, D. J. Fox, T. Keith, M. A. A-Laham, C. Y. Peng, A. Nanayakkara, M. Challacombe, P. M. W. Gill, B. Johnson, W. Chen, M. W. Wong, C. Gonzalez and J. A. Pople, *Gaussian 03*, Gaussian, Inc., Wallingford, CT., 2004.
29 A. D. Becke, *J. Chem. Phys.*, 1993, **98**, 5648.
30 C. T. Lee, W. T. Yang and R. G. Parr, *Phys. Rev. B: Condens. Matter Mater. Phys.*, 1988, **37**, 785.
31 H. Zhou, H. Tamura, S. Takami, M. Kubo, R. Belosloudov, N. Zhanpeisov and A. Miyamoto, *Appl. Surf. Sci.*, 2000, **158**, 38–42.
32 J. A. Dean, *Properties of atoms, radicals, and bonds. Lange's Handbook of Chemistry*, 15th edn, 1999, Section 4, p. 36.
33 A. Sebetci, *Chem. Phys.*, 2008, **354**, 196–201.
34 Q.-M. Ma, Z. Xie, J. Wang, Y. Liu and Y.-C. Li, *Phys. Lett. A*, 2006, **358**, 289–296.
35 S. Datta, M. Kabir, S. Ganguly, B. Sanyal, T. Saha-Dasgupta and A. Mookerjee, *Phys. Rev. B: Condens. Matter Mater. Phys.*, 2007, **76**, 014429.
36 A. V. Arbuznikov and M. Hendrickx, *Chem. Phys. Lett.*, 2000, **320**, 575–581.
37 J. Y. Yuan, H.-G. Xu, Z.-G. Zhang, Y. Feng and W. J. Zheng, *J. Phys. Chem. A*, 2011, **115**, 182–186.
38 K. M. Ervin and W. C. Lineberger, *J. Phys. Chem.*, 1991, **95**, 1167–1177.